6-2024

Hydrothermal synthesis of (C5H14N2)[CoCl4]·0.5H2O: Crystal structure, spectroscopic characterization, thermal behavior, magnetic properties and biological evaluation

Sandra Walha

Noureddine Mhadhbi

Basem F. Ali

Abdellah Kaiba

Ahlem Guesmi

See next page for additional authors

Authors

Sandra Walha, Noureddine Mhadhbi, Basem F. Ali, Abdellah Kaiba, Ahlem Guesmi, Wesam Abd El-Fattah, Naoufel Ben Hamadi, Mark M. Turnbull, Ferdinando Costantino, and Houcine Naïli

Chemical Physics Impact 8 (2024) 100597

Contents lists available at ScienceDirect

Chemical Physics Impact

journal homepage: www.sciencedirect.com/journal/chemical-physics-impact

Full Length Article

Hydrothermal synthesis of $(C_5H_{14}N_2)[CoCl_4]\cdot 0.5H_2O$: Crystal structure, spectroscopic characterization, thermal behavior, magnetic properties and biological evaluation

Sandra Walha [a], Noureddine Mhadhbi [a,b], Basem F. Ali [c], Abdellah Kaiba [d], Ahlem Guesmi [e], Wesam Abd El-Fattah [e], Naoufel Ben Hamadi [e], Mark M. Turnbull [f], Ferdinando Costantino [g,*], Houcine Naïli [a,*]

[a] Laboratory Physico-Chemistry of the Solid State (LR11 ES 51), Department of Chemistry, Faculty of Sciences of Sfax, University of Sfax, B.P. 1171, Sfax 3000, Tunisia
[b] University of Monastir, Preparatory Institute for Engineering Studies of Monastir, Monastir 5019, Tunisia
[c] Department of Chemistry, Al al-Bayt University, Mafraq 25113, Jordan
[d] Department of Physics, College of Science and Humanities in Al-Kharj, Prince Sattam bin Abdulaziz University, Al-Kharj 11942, Saudi Arabia
[e] Chemistry Department, College of Science, Imam Mohammad Ibn Saud Islamic University (IMSIU), Riyadh 11623, Saudi Arabia
[f] Carlson School of Chemistry and Biochemistry, Clark University, Worcester, MA 01610, USA
[g] Department of Chemistry Biology and Biotechnologies, University of Perugia, Via Elce di Sotto 8, Perugia 06123, Italy

ARTICLE INFO

Keywords:
Cobalt (II)
Crystal structure
Hirshfeld surfaces
Magnetic properties
Biological activities

ABSTRACT

The organic-inorganic compound $(C_5H_{14}N_2)[CoCl_4]\cdot 0.5H_2O$, I, was characterized by various physicochemical techniques. The X-ray diffraction analysis revealed that the compound crystallizes in the centrosymmetric space group C2/c of the monoclinic system. The atomic arrangement the Co(II) complex is built from isolated $[CoCl_4]^{2-}$ anions, 1-methylpiperazine-1,4-diium $[C_5H_{14}N_2]^{2+}$ cations and free water molecules. The crystal structure study showed that the cohesion of I is assured through N–H···Cl and N–H···O hydrogen bonds giving birth to a 3-D architecture. Hirshfeld surface analysis revealed that Cl···H/H···Cl and H···H (58.5 and 36.4%, respectively) are the most significant interactions between species. Minor O···H/H···O interactions are also present. The compound was characterized by thermal analysis, TGA-DTA showed the removal of the co-crystallized water before 100 °C and a first mass loss at around 120 °C. Magnetic measurements are in good agreement with isolated, $S = 3/2$, tetrahedral $[CoCl_4]^{2-}$ anions. The negative Weiss constant of -1.35 indicates single-ion anisotropy and very weak antiferromagnetic interactions. UV–visible spectroscopy reveals three weak absorption bands in the visible range due to the d-d electronic transitions typical of the Co(II) tetra-coordinated. A bioassay showed antibacterial activity against the gram negative *Klebsiella pneumonia* and gram positive *Bacillus ceureus, Listeria monocytogenes*, and *Micrococcus lutues*.

1. Introduction

The hydrothermal method was originally the domain of geochemists and mineralogists interested in the simulation of mineral formation [1]. However, the hydrothermal technique has recently been adopted for the synthesis of a wide variety of metastable materials [2] and can be considered as a special case of chemical transport reactions [3–6]. Metal coordination of organic-inorganic compounds is not only recognized as an important factor in drug design and medicinal inorganic chemistry research, but is also being considered in enhancing drug bioactivity. For example, complexes of cobalt have been of great research interest due to their unique structural topologies, structural diversity and the development of new pharmaceutical drugs [7–11]. They may also provide very good catalysts [12]. Cobalt appears to be a reasonable choice for bioactive materials because it is an essential element present in the body in the vitamin B_{12} complex; consequently, it maintains the normal functioning of the nervous system and can regulate the synthesis of DNA [13]. The coordination number of the metal ion in a complex can be six (octahedral) [14–16], five (trigonal bipyramidal or square pyramidal) [17–19] and four (tetrahedral) [20–22]. More particularly, hybrid

* Corresponding authors.
E-mail addresses: ferdinando.costantino@unipg.it (F. Costantino), houcine.naili@fss.rnu.rn (H. Naïli).

https://doi.org/10.1016/j.chphi.2024.100597

Available online 3 April 2024

compounds of the general formula $A[MX_4]^{2-}$, where M is a transition metal, X is Cl or Br and A is an organic cation, are an interesting area of chemistry and extensively studied using different spectroscopic methods in the literature [23–25]. Cobalt complexes have also been explored to study their thermal [26–28] and magnetic [29] properties. A variety of amines has been employed previously in the preparation of halidocobaltates, including aliphatic, aromatic and cyclic amines [30–32]. Previous studies have shown that hybrid inorganic-organic compounds containing piperazine and its derivatives exhibit a wide range of biological activities including anticancer, antimicrobial, antiviral and antimalarial activity [33,34] making it a desirable ancillary ligand to explore properties of new inorganic-organic hybrid structures. In particular, we used 1-methylpiperazine combined with Co(II) as the metal ion source which has importance in catalytic activity, magnetic behavior and biological activity; in addition, the large flexible coordination environment of Co(II) provide unique opportunities for the formation of extended organic-inorganic compounds [35–39]. Considering the attractive attributes of halidocobaltate(II) anions, we report here the hydrothermal synthesis and crystal structure of 1-methylpiperazine-1, 4-diium tetrachloridocobaltate(II) hemihydrate, I, as well as the Hirshfeld surface analysis, thermal behavior, antibacterial activity and magnetic proprieties.

2. Experimental section

2.1. Materials

Cobalt (II) chloride hexahydrate ($CoCl_2{\cdot}6H_2O$), hydrochloric acid (HCl; 37%), and 1-methylpiperazine dihydrochloride ($C_5H_{14}N_2.2HCl$) were purchased from Sigma-Aldrich and used without further purification.

2.2. Synthesis

Attempts to prepare the title compound by the slow evaporation method resulted the isolation of crystals of methylpiperazine-1,4-diium dichloride. For this reason, we used the hydrothermal method for the synthesis of I.

The synthesis of I was carried out in home-built Teflon-lined stainless steel pressure bombs of 120 mL maximum capacity. A mixture of cobalt (II) chloride hexahydrate (0.47 g, 2.0 mmol) and 1-methylpiperazine dihydrochloride (0.69 g, 4.0 mmol) were dissolved together in 30 mL of deionized water and hydrochloric acid (pH = 3). The mixture was placed in a Teflon-lined autoclave that was then sealed and heated to 160 °C for 3 days. It was then cooled to room temperature in a water bath. The autoclave was opened in air, and products were recovered through filtration. Transparent blue, plate crystals with suitable dimensions for crystallographic study were recovered. The crystals were washed several times with distilled water and dried in open air. The yield of the reaction was 97%; the obtained mass of the sample was 0.614 g. Elem. microanal. Obsd for I (calcd): C, 10.28 (10.08); H, 3.17 (3.02); N, 5.14 (4.97). (IR, KBr, cm^{-1}): ν (H_20), 3506 s; δ (N-H^+), 1460 m; ν (C—N), 1180 m, (s = strong, m = medium). The synthesis of the hybrid material has been carried out by using the following reaction scheme (Scheme 1):

Table 1
Crystal Data and Structure Refinement for Compound $(C_5H_{14}N_2)[CoCl_4]{\cdot}0{\cdot}5H_2O$.

empirical formula	$(C_5H_{14}N_2)[CoCl_4]{\cdot}0.5H_2O$
formula weight	623.84
temperature (K)	293(2)
crystal system	Monoclinic
space group	C2/c
a (Å)	14.3430 (7)
b (Å)	12.7870 (14)
c (Å)	13.7880 (6)
ß (deg)	102.744 (4)
V(Å^3)	2466.5 (3)
Z	4
Dcalc, (g·cm^{-3})	1.686
λ(MoKα) (Å)	0.71073
crystal form, color	plate-blue
crystal size (mm)	0.47 × 0.11 × 0.08
μ (mm^{-1})	2.22
Θ ranges (deg)	3.03 – 32.01
absorption correction	Multi-scan
refinement method	SHELXL
F(000)	1264
goodness-of-fit on F2	1.206
R_1, wR_2 [$I > 2\sigma(I)$]	0.034, 0.055
no. parameters	128
transmission factors	0.747–0.834
(Δρ)min, (Δρ)max, eÅ^{-3}	−0.43 and 0.56

2.3. X-ray data collection

A suitable crystal was mounted on a D8 VENTURE Bruker AXS diffractometer and studied using graphite monochromated Mo Kα radiation (λ = 0.71073 Å) through the program APEX3 [40]. Data collection, data reduction and analysis were processed using SAINT [41]. Empirical absorption corrections of the multi-scan type were performed using the SADABS program [42]. The crystal structure was solved in the monoclinic crystal class, space group C2/c, according to the automated search for space group available in Wingx [43]. The molecular solid state structure was solved by direct methods using the SHELXT software package [44] and refined by full-matrix least-square methods on F^2 with SHELXL-2015 [45].The main crystallographic data and refinement parameters are presented in Table 1.

2.4. Thermal analysis

The simultaneous TG–DTA analysis of I was carried out in air at a heating rate of 5 °C/min over the temperature range 25–550 °C on a 3.84 mg sample.

2.5. Spectroscopic measurements

IR spectrum of 4PPHP was recorded in the region 4000–400 cm^{-1} by means of pellets containing the sample in question and KBr as a dispersant with 1.0 cm^{-1} resolution with a Bruker Vertex 80 V FT-IR spectrometer All the bonds were assigned by comparison with the spectrum of other compounds, at room temperature and in the 400–4000 cm^{-1} frequency range. The optical absorption spectrum of the

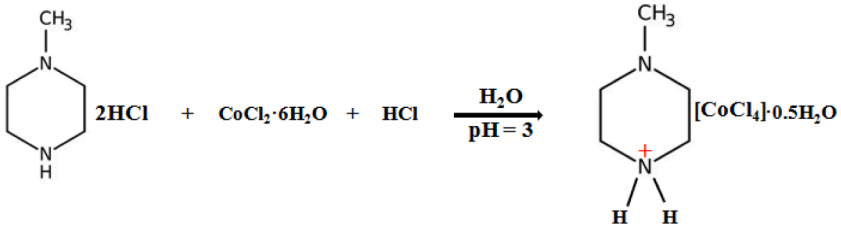

Scheme 1. Synthesis of complex $(C_5H_{14}N_2)[CoCl_4]{\cdot}0{\cdot}5H_2O$.

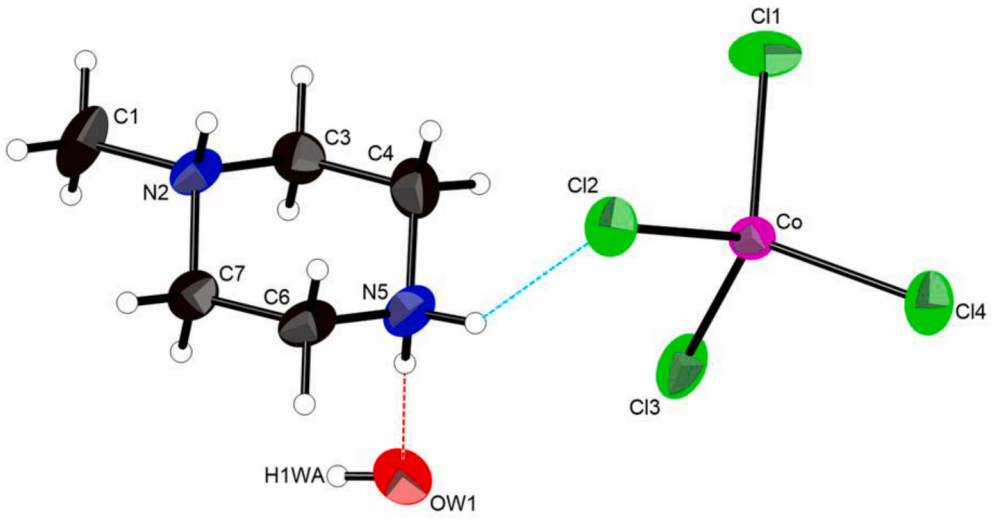

Fig. 1. The asymmetric unit of I with atom labeling scheme. Displacement ellipsoids are drawn at 50% probability level. Hydrogen atoms are shown as spheres of arbitrary radius. Hydrogen bonding interactions are shown as dashed lines.

films was recorded at room temperature in the wavelength range from 200 nm to 800 nm using a conventional UV–visible absorption spectrometer.

2.6. Magnetic measurements

Magnetic properties of a powdered sample of I were measured using a Quantum Design MPMS-XL SQUID magnetometer. The moment was measured using magnetic fields from 0 to 50 kOe at 1.8 K. Several data points were recollected as the field returned to zero to look for hysteresis effects. None were observed. Magnetic susceptibility measurements in the range of 1.8–310 K were carried out in an applied magnetic field of 1000 Oe The data were corrected for the diamagnetic contributions of the constituent atoms, estimated via Pascal's constants [46] and for the background signal of the sample holder (measured independently). Data were fit using the Hamiltonian $\hat{H} = -2\sum_{A,B} J_{AB}\, \hat{s}_A.\hat{s}_B$.

2.7. Biological study

2.7.1. Antimicrobial activity

Antimicrobial activity was tested against two Gram negative bacteria [*Escherichia coli* and *Klebsiella pneumonia*] and three Gram positive bacteria [*Bacillus ceureus, Listeria monocytogenes and Micrococcus luteus*]. Before use, all microorganisms were stocked in appropriate conditions and regenerated twice. Antimicrobial activity assays were performed according to the method described by the disk diffusion method [47–49].

The test microorganisms were dispersed on appropriate solid medium plates and cultured overnight at 37 °C. After 24 h, five loops of pure colonies were placed in a test tube with physiological saline solution for each bacterial strain and controlled to the 0.5 McFarland turbidity criteria. Sterile cotton was dipped in the bacterial suspension and the agar plates were streaked three times. Each time the plate was rotated at an angle of 60°. Finally, the swab was rubbed over the edge of the plate. Sterile filter paper discs were placed on inoculated plates. In order to prove the activity of the synthesized complexes, DMS solutions concentrated at 150 mg/mL of the salt $CoCl_2$, 1-methylpiperazine and the cobalt complex were tested against the used bacteria. As a positive reference, ampicillin was utilized. The sizes of the inhibitory zones were measured with a ruler with an accuracy of 0.5 mm.

2.7.2. Antioxidant studies

Diphenylpicrylhydrazyl (DPPH) and 2,2-azino-bis(3-ethylbenzothiazoline-6-sulfonic acid)) (ABT) were the two assays used to examine the *in-vitro* antioxidant activity of $(C_5H_{14}N_2)[CoCl_4]\cdot 0.5H_2O$ and 1-methylpiperazine dihydrochloride. Using the methodology [49] as outlined in [50], the DPPH activity of $(C_5H_{14}N_2)[CoCl_4]\cdot 0.5H_2O$ and 1-methylpiperazine dihydrochloride was investigated. In a nutshell, distinct quantities of 1-methylpiperazine dihydrochloride (0.1 and 2.5 mg/ml) and $(C_5H_{14}N_2)[CoCl_4]\cdot 0.5H_2O$ (0.5 to 50 mg/ml) were synthesized. On methanol, the two tested compounds were dissolved. One milliliter each of DPPH methanol solution (0.1 mM) and $(C_5H_{14}N_2)[CoCl_4]\cdot 0.5H_2O$ were combined with one milliliter of 1-methylpiperazine dihydrochloride solution. Following a 30 min incubation period at room temperature and depending on obscurity, 517 nm was used to test absorbance. Every sample was examined three times. The following formula was used to calculate the scavenging activity: Scavenged activity (%) of DPPH radicals $= [(A_0 - A_1)/A_0] \times 100$. where A_0 denotes the blank's absorbance and A_1 is the absorbance measured with 1-methylpiperazine dihydrochloride or $(C_5H_{14}N_2)[CoCl_4]\cdot 0.5H_2O$ present. The ABTS test is based on how the ABTS cation changes color in response to an antioxidant. Indeed, when ABTS reacts with potassium persulfate, it transforms into its blue radical cation. The colorless form of ABTS is often produced when the cation of ABTS reacts with an antioxidant. Spectrophotometry is used to measure the color change. To create a stock solution for the ABTS test, an equal volume of 2.45 mM potassium persulfate solution and 7 mM ABTS solution were combined. An equal volume of the stock solution and 50% methanol are mixed to create a fresh working solution before each essay, which is then allowed to sit at room temperature in the dark for 12 h For $(C_5H_{14}N_2)[CoCl_4]\cdot 0.5H_2O$, various concentrations ranging from 10 to 20 mg/ml and from 0.1 to 10 mg/ml for 1-methylpiperazine dihydrochloride were generated. A solution of ABTS (three milliliters) was mixed with 300 microliters of $(C_5H_{14}N_2)[CoCl_4]\cdot 0.5H_2O$ and 1-methylpiperazine dihydrochloride. The mixture was incubated for six minutes at room temperature and in the dark. The following formula was used to determine the scavenging activity: Scavenged activity (%) of ABTS radicals $= [(A_0 - A_1)/A_0] \times 100$. where A_1 is the absorbance determined while the tested chemical is present, and A_0 is the absorbance of the blank, or the reaction mixture without the tested molecule.

3. Results and discussion

3.1. Molecular structure and supramolecular features of I

The title salt, I, crystallizes in a monoclinic space group, *C2/c*. The

Table 2
Selected bond distances (Å) and angles (°) in $(C_5H_{14}N_2)[CoCl_4]\cdot 0.5H_2O$.

Tetrahedron around Co^{II}	Within the organic cation
Co-Cl1 2.2658(6)	C1-N2 1.496(2)
Co-Cl2 2.2978(5)	N2-C3 1.497(2)
Co-Cl3 2.2657(5)	N2-C7 1.496(2)
Co-Cl4 2.2543(5)	C3-C4 1.512(3)
Cl1-Co-Cl3 109.06 (2)	C4-N5 1.496(3)
Cl1-Co-Cl4 112.00(3)	N5-C6 1.490(3)
Cl1- Co-Cl2 106.42(2)	C6-C7 1.505(3)
Cl2- Co -Cl3 106.74(2)	C1-N2-C7 111.46(2)
Cl2- Co-Cl4 112.81(2)	C1-N2-C3 110.66(3)
Cl3- Co-Cl4 109.60(2)	C7-N2-C3 110.06(3)
	N2-C3-C4 111.57(3)
	N5-C4-C3 110.21(3)
	C6-N5-C4 111.34(15)
	N5-C6-C7 109.92(16)
	N2-C7-C6 110.78(16)

asymmetric unit consists of one $[CoCl_4]^{2-}$ dianion, one 1-methylpiperazine-1,4-diium dication, and one-half OH_2 unit (having C_2 crystallographic symmetry), Fig. 1. The $[CoCl_4]^{2-}$ anions have a slightly distorted tetrahedral coordination geometry as evident from the Cl—Co—Cl angles in the range 106.42(2)–112.81(2)° being closer to 109.5°. Moreover, the Co—Cl bond distances are in the range 2.254(5)–2.297(6) Å, Table 2. Bond distances and angles are typical and fall within reported values for the corresponding $[CoCl_4]^{2-}$ containing salts $(C_6H_9N_2)_2[CoCl_4]$ [51] and (3-(chloromethyl)pyridinium)$_2CoCl_4$ [52] and noted in many other structures [20,24,25]. As far as the dication is concerned, the 1-methylpiperazine-1,4-diium ring adopts a typical chair conformation with average C—C and C—N bond distances of 1.508(2) and 1.497(3) Å, respectively, which are compatible with other 1-methylpiperazine-1,4-diium rings $(C_5H_{14}N_2)[ZnCl_4]\cdot 0.5H_2O$ [53] and $(C_5H_{14}N_2)[Ni_2Cl_4(H_2O)_6]Cl_2$ [54]).

In the structure of I, the water molecules operate as linking building blocks between the $[CoCl_4]^{2-}$ anions and 1-methylpiperazine-1,4-diium cations (Fig. 1). The crystal packing in I is shown in Fig. 2. There are segregated anion stacks and cation•••H_2O layers. The anion stacks run parallel to the *c*-axis while the cation•••H_2O layers are parallel to the *ac*-plane (Fig. 2). The organic cations not only play a space-filling and charge-compensating role but also are intimately involved in structural propagation along with the water molecules which strengthen the cohesion of the structure by linking the organic and inorganic cations extending into three-dimensional supramolecular architecture via hydrogen bonds. The 2-dimensional cation•••H_2O layers (Fig. 3) are composed of N—H•••O—H_2 hydrogen bonding [N5•••OW1 = 2.909(2) Å] which runs parallel to the *ac* plane. The discrete $[CoCl_4]^{2-}$ anion stacks and the cation•••H_2O layers are connected through additional HO—H•••Cl—Co and N—H•••Cl—Co interactions [N5•••Cl2 = 3.358 (3), N2•••$Cl1^{i}$ = 3.189(4) and OW1•••$Cl2^{ii}$ = 3.280(2) Å; Symmetry codes: (i) $-x + 1/2, -y + 1/2, -z + 1$; (ii) $x, -y + 1, z - 1/2$], Fig. 3, forming an alternating $R_6^4(12)$ ring motif, Fig. 4. The combination of anion stacks and 2-D cation•••H_2O layers intermolecular interactions generates a fascinating 3-dimensional network structure. Hydrogen-bonding parameters are summarized in Table 3.

It is worth mentioning that the title salt is isomorphous with the tetrachloridozincate(II) analogue [53]. The structure of the zinc

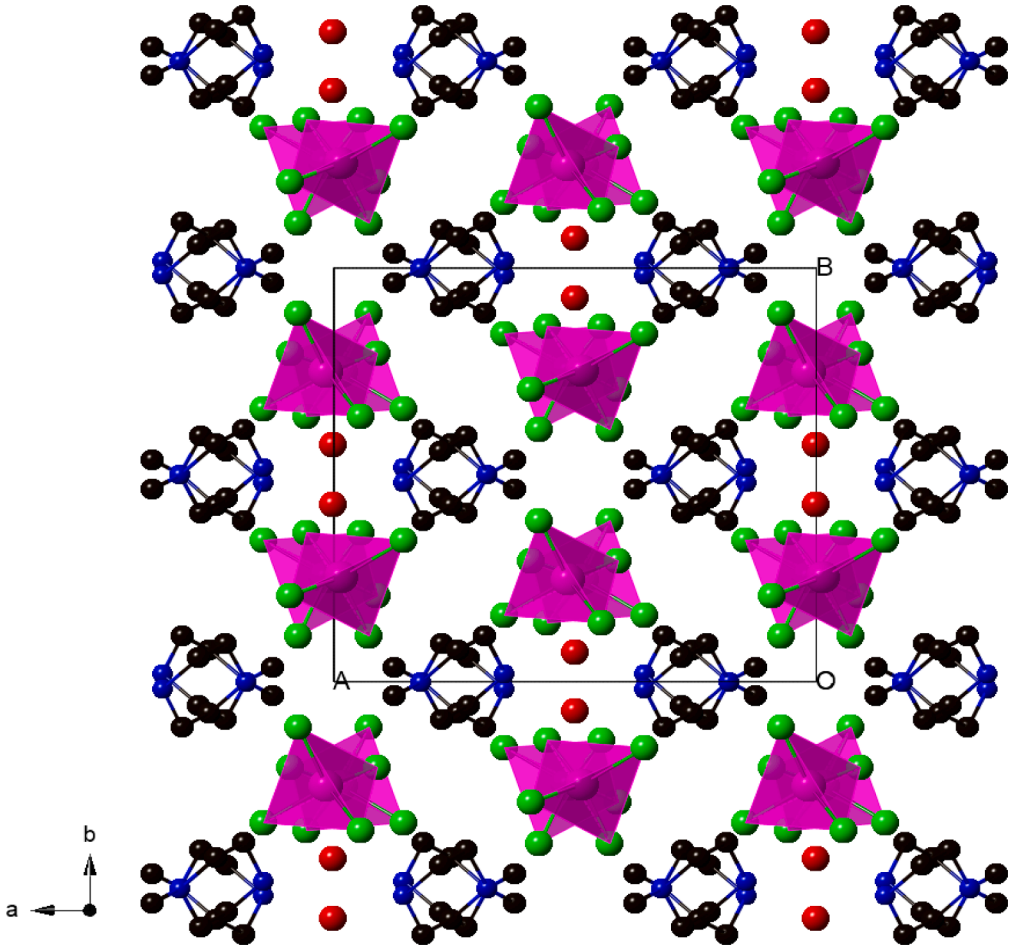

Fig. 2. The crystal packing in I. The anions are arranged in discrete stacks of $[CoCl_4]^{2-}$ species, parallel to the *c*-axis, separated by domains containing the 1-methylpiperazine-1,4-diium cations and H_2O. Hydrogen atoms omitted for clarity.

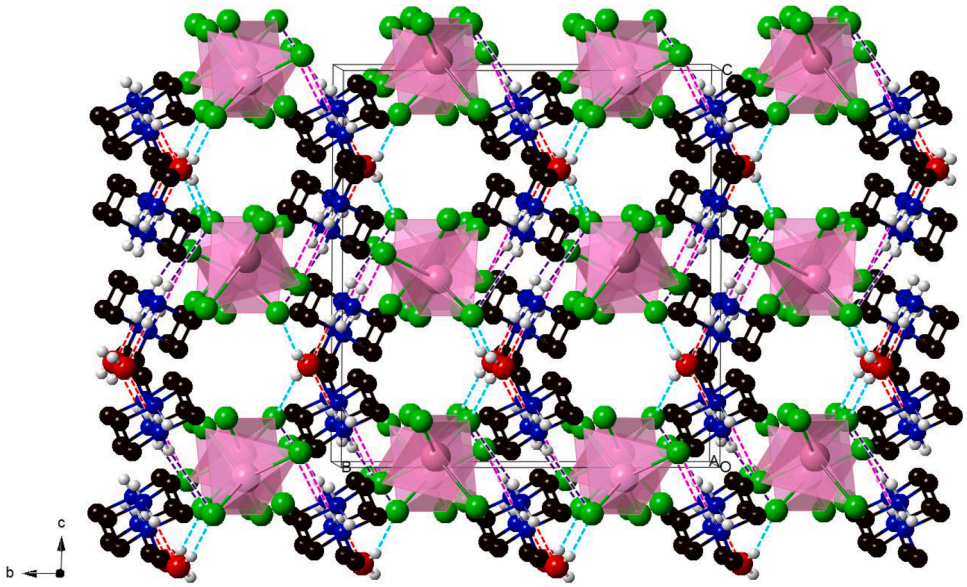

(a)

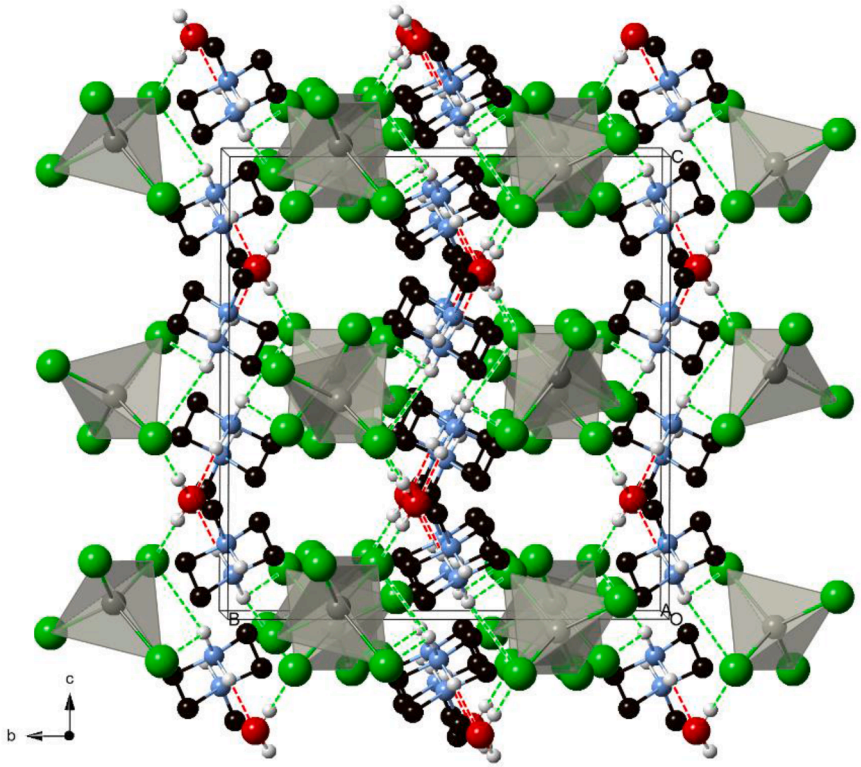

(b)

Fig. 3. (a) Partial packing view with N—H•••O—H_2 (red dashed lines), HO—H•••Cl—Co (blue dashed lines) and N—H•••Cl—Co (black and pink dashed lines) hydrogen bonding interactions; (b) Similar packing view of the isomorphous tetrachloridozincate(II) derivative showing N—H•••O—H_2 (red dashed lines), HO—H•••Cl—Co and N—H•••Cl—Co (green dashed lines) hydrogen bonding interactions. Hydrogen atoms not involved in interactions are omitted for clarity.

derivative shows a similar supramolecular structure, as illustrated in Fig. 3b. In the lattice, the $ZnCl_4$ stacks are linked by donor water molecules into chains along *c*-axis by O—H•••Cl hydrogen bonds. The water molecules again act as acceptors and connect to the dications *via* N—H•••O hydrogen bonds, Fig. 3b, resulting in an overall packing identical to that of the title compound, Fig. 3a. The stability of this type of lattice is evident by the crystallization of these two isomorphous derivatives. The related anhydrous CuX_4^{2-} complexes have also been reported but in different lattice types [55,56].

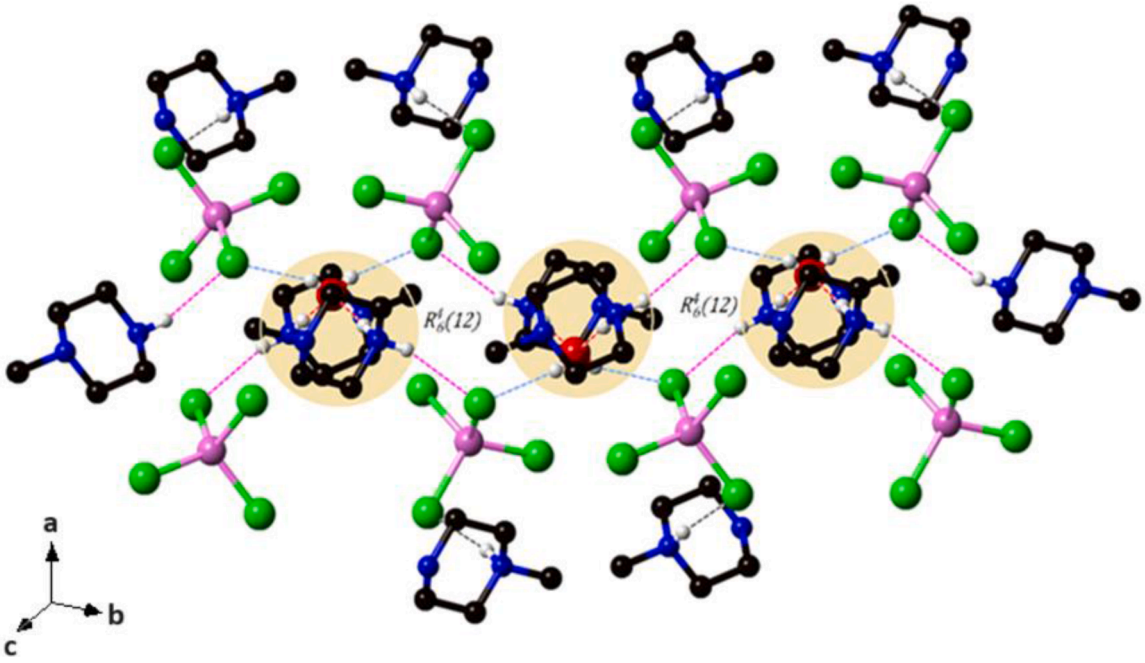

Fig. 4. One layer showing the anions and cations•••water interactions forming alternating $R_6^4(12)$ ring motifs. Cation•••water slabs are highlighted in cream. Hydrogen atoms not involved in interactions are omitted for clarity.

Table 3
Hydrogen bonding parameters for compound $(C_5H_{14}N_2)[CoCl_4]\cdot 0.5H_2O$.

D–H···A	D–H (Å)	H···A (Å)	D···A (Å)	D–H···A (°)
N5–H5B …Cl2	0.87(3)	2.64(3)	3.358(19)	141(2)
N5 –H5A …OW1	0.89(2)	2.02(3)	2.909(2)	176(2)
N2 –H2 …Cl1^{i}	0.86(2)	2.35(2)	3.189(16)	165.4 (19)
OW1 –H1WA …Cl2^{ii}	0.76(2)	2.55(2)	3.280(2)	162(3)

Symmetry codes:.
(i) -*x* + 1/2, -*y* + 1/2, -*z* + 1; (ii) x, -*y* + 1, z-1/2.

3.2. Hirshfeld surface analysis

The Hirshfeld surface is representative of the region in space where molecules come into contact with each other, allowing the analysis of the chemical nature of intermolecular interactions in the crystal. Hirshfeld surface analysis and 2D fingerprint plots for I were created using Crystal Explorer 21.5 [57]. The Hirshfeld surface mapped over d_{norm} is shown in Fig. 5a. The 2D fingerprint plots, illustrated in Fig. 5 (b–e), reveal that the most significant contacts are Cl•••H/H•••Cl (58.5%, Fig. 5c) and H•••H (36.4%, Fig. 5d). Other minor O•••H/H•••O (3.3%, Fig. 5e) interactions are also present.

The interatomic contacts H•••Cl/Cl•••H have the greatest contribution to the Hirshfeld surface (58.5%), attributed to the N•••H/Cl and C•••H/Cl hydrogen-bonding interactions and represented by two sharp symmetric spikes in the two-dimensional fingerprint maps, with a maximum d_e+d_i 2.30 Å (Fig. 5c). This value is less than the sum of van der Waals radii of chlorine (1.75 Å) and hydrogen (1.09 Å) atoms; it confirms that the inter-molecular contact is considered as being close contact. In addition, O···H/H···O interactions constitute 3.3% of the total area of Hirshfeld surface of compound I.

3.3. Thermal behavior

Simultaneous TG-DTA curves of I in the temperature range 50–500 °C with a heating rate of 5 °C /min are depicted in Fig. 6. The examination of the TG curve shows that the first weight loss is observed at 90 °C, and corresponds to the departure of the water molecules (observed weight loss = 1.45%; calculated weight loss = 1.6%) giving rise to the anhydrous phase $(C_5H_{14}N_2)[CoCl_4]$. This phenomenon is accompanied by an endothermic peak observed on the DTA curve at 95 °C. The second weight loss occurring between 120 and 200 °C is due to the departure of 2HCl molecules (observed weight loss, 11.92%; theoretical weight loss 11.8%). This phenomenon is accompanied by endothermic peaks observed on the DTA curve at 150 and 180 °C. The second weight loss occurring between 190 and 370 °C is due to the degradation of the organic cation from the compound (observed weight loss = 18.9%; calculated weight loss = 18.45%). This decomposition process is accompanied by a endothermic peaks observed at 340 °C and 360 °C. The last step of the decomposition corresponds to the formation of the cobalt oxide CoO via atmospheric moisture.

3.4. Magnetic properties

Magnetization measurements for I at 1.8 K as a function of applied field (see Fig. S1, ESI) show a steady rise to ~ 14,000 emu/mol at 50 kOe (the maximum applied field) in good agreement with the expected saturation moment (~17,000 emu/mol) for an $S = 3/2$ ion [58,59]. The magnetic susceptibility increases monotonically with descending temperature (see Fig. S2, ESI) and no sign of a maximum is observed. A Curie-Weiss plot of the data (Fig. 7) yielded a Curie Constant (C) of 2.61 (1) emu-K/mol-Oe in good agreement with the expected value for a tetrahedral Co(II) complex [59] and a Weiss constant, θ, of −1.35(5). The negative Weiss constant indicates the presence of single-ion anisotropy, antiferromagnetic exchange, or a combination thereof. The χT(T) data were fit to a model including single-ion anisotropy only, yielding C = 2.59(2) emu-K/mol-Oe and D = 12.1(6) K, suggesting a modest single-ion anisotropy. The data were also fit to the single-ion anisotropy model incorporating a Curie-Weiss term to account for possible exchange between the $CoCl_4^{2-}$ ions (see Fig. 7) [60]. This yielded C = 2.582(2) emu-K/mol-Oe, D = 10.20(8) K and θ = −0.25(3) K. The small modification to D and negligible Weiss constant indicate that the temperature dependent behavior results almost completely from single-ion anisotropy as is typical of such materials [54–56].

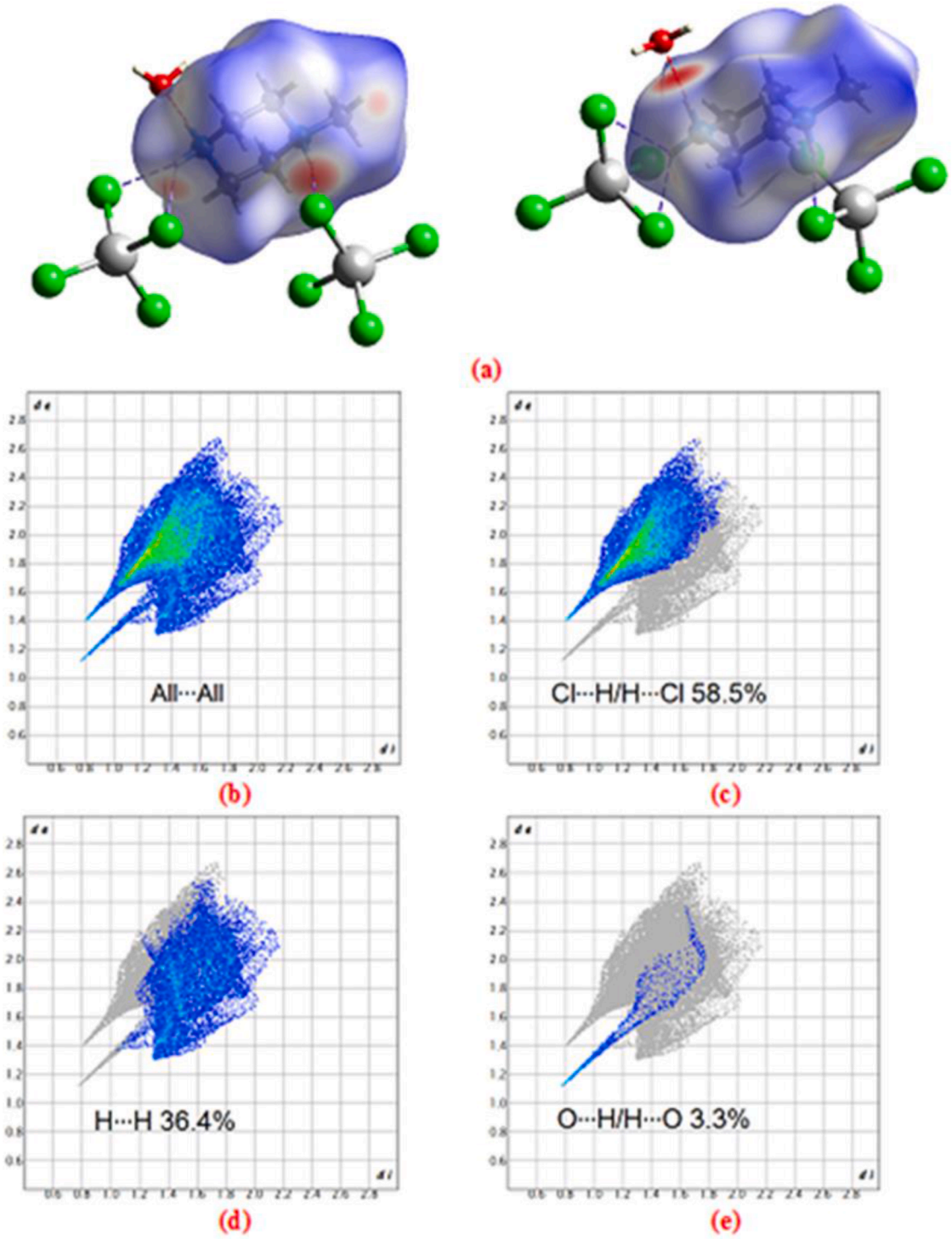

Fig. 5. View of the Hirshfeld surface of I mapped over d_{norm}. The two-dimensional finger print plots of : (b) all···all interactions, and delineated into (c) Cl···H/H···Cl; (d) H···H; (e) O···H/H···O interactions.

3.5. IR spectroscopy

In order to give more information on the crystal structure, we have studied the vibrational properties of I using infrared absorption spectroscopy. The IR spectrum, (presented in Fig. S3, ESI), shows several absorptions bands. All assignments of the observed vibrational modes are made by comparison with previous work performed in homologous compounds [61,62]. The bands situated at 3506, 3220 and 1570 cm^{-1} are assigned to the stretching and deformation vibration of the water molecule. The remaining two bands observed at 2800 and 2676 cm^{-1} are attributed to the asymmetric and symmetric N—H stretching.

The bending vibrations of N—$H^{+}$are observed around 1460 and 1505 cm^{-1} and the other absorption bands observed at 2995 and 1180 cm^{-1} are proposed to be the stretching and bending vibrations of C—H, respectively. Weak bands situated at 2610, 2500 and 2409 cm^{-1} are assigned to stretching of NH_2^+ groups involved in hydrogen bonds (N—H•••Cl). These findings support the composition and structure of compound I, particularly the presence of 1-methylpiperazine-1,4-diium.

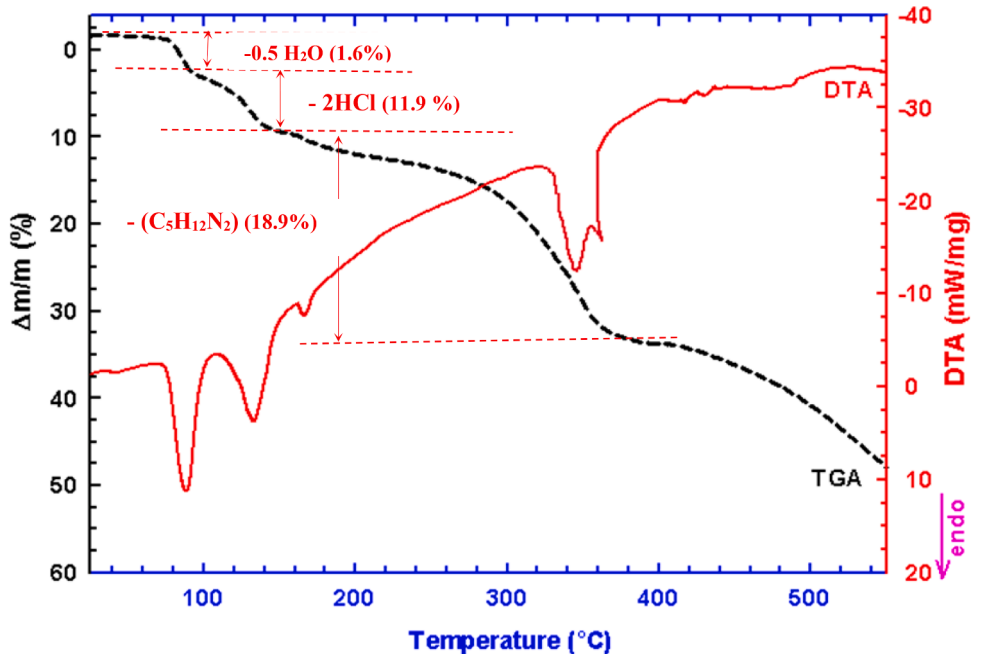

Fig. 6. Simultaneous thermogravimetric analysis and differential thermal analysis scan for the decomposition of I under flowing air with a heating rate of 5 °C/min between 25 and 550 °C.

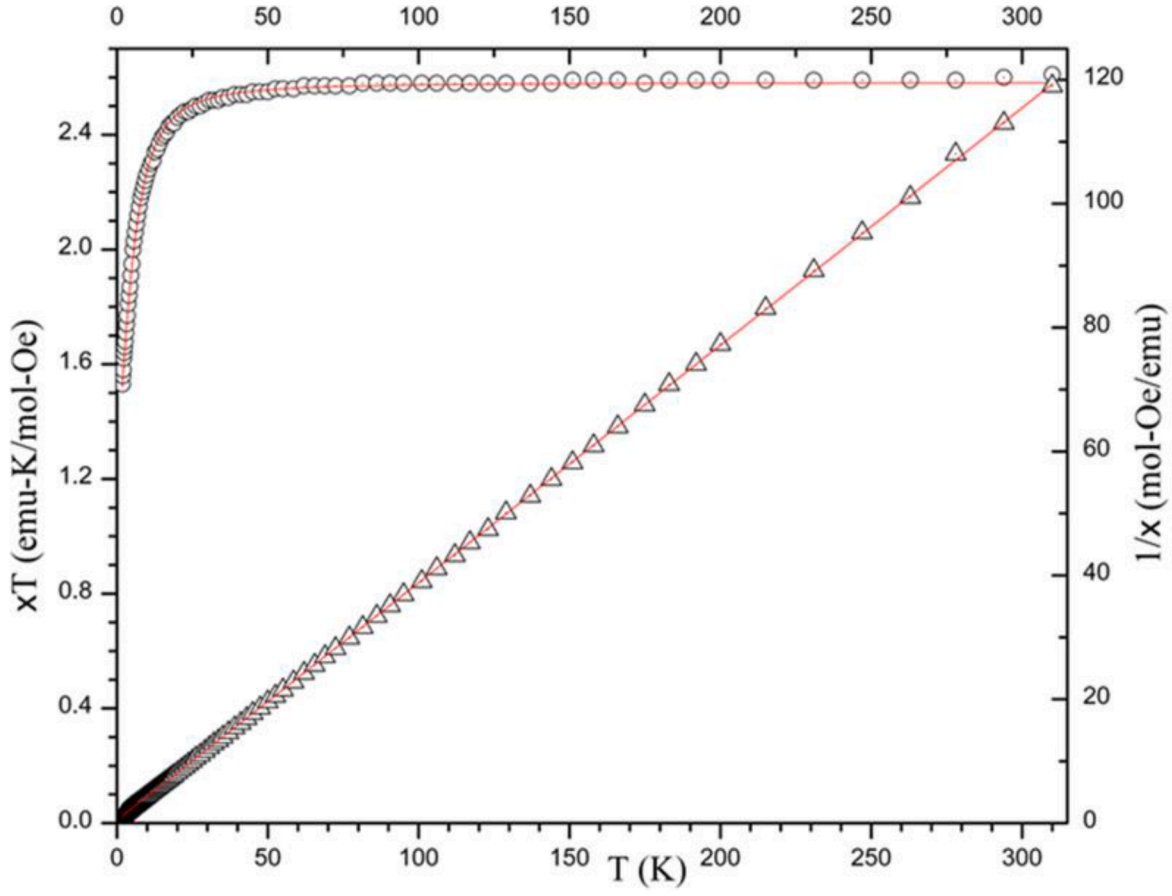

Fig. 7. Plot of χT(T) and 1/χ (T) in the temperature range from 1.8 to 300 K for I. The solid lines represent the Curie–Weiss fit of the data.

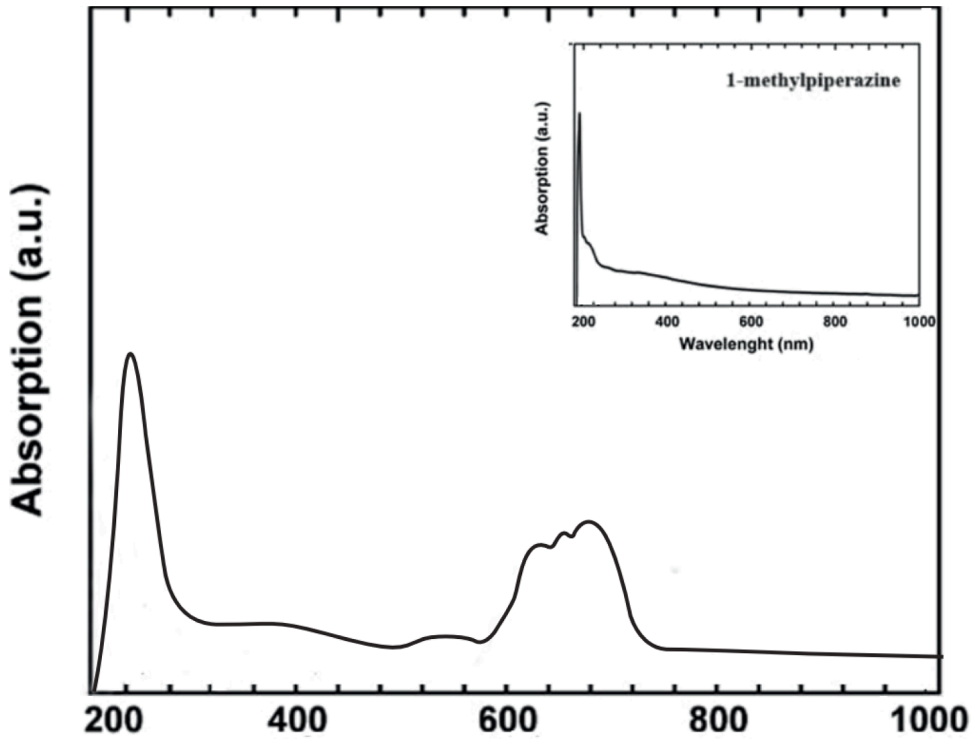

Fig. 8. Optical spectrum of $(C_5H_{14}N_2)[CoCl_4]{\cdot}0.5H_2O$.

Table 4
Diameters of inhibitory zones for solutions of the salt $CoCl_2$, 1- methylpiperazine and compound I ; Inhibition zones: ++++ >25 mm ; +++: >15 mm; ++: 10-15 mm, +: <5 mm :.

		Zones of growth inhibition surrounding the disc (mm)		
Name of bacterial strains	$CoCl_2$	1-methylpiperazine	Compound I	Ampicilin
E. coli G(-)	–	++	+	+
Klebsiella pneumonia G(-)	–	++	+	+
Bacillus crereus G(+)	++	–	++	+++
Listeria monocytogenes G (+)	++	–	+++	++++
Micrococcus luteus G (+)	++	–	++	++++

- inactive.

3.6. UV–vis spectroscopy

The UV-visible absorption of compound I and 1- methyl piperazine in DMSO is illustrated in Fig. 8. The spectrum of 1-methylpiperazine shows one band at $\lambda = 220$ nm, indicates the $n \rightarrow \pi^*$ transition of the organic cation. As can be seen at the higher wavelength region of the spectrum on Fig. 8, the shape and position of the observed features are typical of any tetrahedral-like Co-complex spectrum and are very similar to that obtained for other cobalt (II) bromide or cobalt (II) chloride compounds found in literature [63–65]. In fact, they are discernible with three peaks located at 620, 650 and 680 nm and are generally assigned to the three well known spin allowed d-d electronic transitions ($^4T_{1g}(F) \rightarrow {}^4T_{1g}(P)$, $^4T_{1g}(F) \rightarrow {}^4A_{2g}(F)$ and $^4T_{1g}(F) \rightarrow {}^4T_{2g}$ (F), respectively) within the $[CoCl_4]^{2-}$ inorganic parts.

3.7. Biological activities

3.7.1. In-vitro antimicrobial activity

We have continued our studies of the antibacterial activity of organic–inorganic hybrid metal(II) halides with derivatives of piperazine, including I and the zinc compoud recently published [66]. The antibacterial tests were performed against three Gram-positive and two Gram-negative bacteria. The three current compounds ($CoCl_2$, 1-methylpiperazine and compound I) were effective against the tested bacteria with variable ranges of diameters of inhibitory zones. Referring to the literature, complexes based on cobalt are found to be very effective against bacteria, in particular Gram-positive bacteria [67,68]. According to the results presented in Table 4, compound I was found to have a moderate activity against the gram- positive bacteria, while it showed weak activity against the gram-negative strains. The weak antibacterial activity against Gram-negative bacteria was ascribed to the presence of an outer membrane which can directly or indirectly cause metabolic dysfunction and finally lead to bacterial death [69]. The cobalt compound I was found to have a significant antibacterial activity against the Gram-positive bacteria tested compared to Gram-negative bacteria (Table 4). Indeed, for Gram-positive bacteria, the largest inhibition diameter (20.66 (4) mm) is recorded in *Listeria monocytogenes* by I. According to Table 4, the complex exhibited the same activity against this bacterium as $CoCl_2$. For the tested Gram-positive bacteria, 1-methypiperazine was not effective against any of them (the diameter of inhibition did not exceed 10 mm). Compared to ampicillin, compound I has the same diameter inhibition zones (12 mm) against *Klebsiella pneumonia*. For the Gram-positive bacteria, Table 4 indicates that the complex is no better than the individual components, the values are the same as $CoCl_2$ except for *Listeria monocytogenes* where it is simply the sum of the free amine activity and the $CoCl_2$ activity, while for the Gram-negative bacteria, the complex is actually worse than the amine itself, which might suggest that protonating the nitrogen atoms inhibits the anti-bacterial activity. It has been reported that the antibacterial activity of a complex is influenced by its stability. The lower stability of compound I, the greater of the antibacterial activity. This may be caused by the presence of more free ions in the solution, which can enhance the cooperative interaction between the metal ions and the ligands [70,71]. Indeed, the antimicrobial results suggested that Co-complex is never more effective than the sum of the components, and sometimes less.

Table 5
Scavenging activity of 1-methylpiperazine dihydrochloride and $(C_5H_{14}N_2)[CoCl_4]\cdot 0.5H_2O$ in both DPPH and ABTS test.

Parameter	$(C_5H_{14}N_2)[CoCl_4]\cdot 0.5H_2O$	1-methylpiperazine dihydrochloride
DPPH IC_{50} (mg/mL)	43.3 ± 0.01	3.56 ± 0.05
ABTS IC_{50} (mg/mL)	16.21 ± 0.03	1.07 ± 0.06

Abbreviations: DPPH: 1,1-Diphenyl-2-Picrylhydrazyl radical scavenging capacity; ABTS: (2,2-azino-bis(3- ethylbenzothiazoline-6-sulfonic acid)) ABTS; IC_{50}: the concentration able to inhibit 50%.
The tests were run in triplicate and data are expressed as mean and standard error of the mean (mean ± SEM). Statistical comparisons were performed using ANOVA followed by Newman-Keuls post hoc test.

3.7.2. Antioxidant assay

The DPPH test results showed that $(C_5H_{14}N_2)[CoCl_4]\cdot 0.5H_2O$ had a much higher ($p < 0.05$) scavenging activity ($IC_{50} = 43.3 \pm 0.01$ mg/ml) than 1-methylpiperazine dihydrochloride ($IC_{50} = 3.56 \pm 0.05$ mg/ml) (Table 5). The ABTS test results validated the DPPH test results. In fact, the 1-methylpiperazine dihydrochloride ($IC_{50} = 1.07 \pm 0.06$ mg/ml) was almost sixteen times lower than the $(C_5H_{14}N_2)[CoCl_4]\cdot 0.5H_2O$ (16.21 ± 0.02 mg/ml). According to our findings, substances that scavenge free radicals include $(C_5H_{14}N_2)[CoCl_4]\cdot 0.5H_2O$ and 1-methylpiperazine dihydrochloride. Nevertheless, both ABTS test and DPPH test revealed that $(C_5H_{14}N_2)[CoCl_4]\cdot 0.5H_2O$ scavenging activity is significantly higher than the 1-methylpiperazine dihydrochloride. This result can be explained by the increased proton diffusion ability of $(C_5H_{14}N_2)[CoCl_4]\cdot 0.5H_2O$ as well as the presence of more reactive sites in its structure, which could be proton donors or electron acceptors.

4. Conclusion

In the present work, we have hydrothermally synthesized and characterized a new cobalt (II) compound, 1-methylpiperazine-1,4-diium tetrachloridocobaltate(II) hemihydrate. This hybrid material exhibits a layered inorganic-organic structure stabilized through extensive O/N–H•••Cl/O hydrogen bonding. Hirshfeld surface analysis revealed that Cl•••H/H•••Cl and H•••H contacts are the most significant interspecies interactions along with minor contribution from O•••H/H•••O interactions. The thermal decomposition of the crystals proceeds through three stages giving rise to cobalt (II) oxide as the final product. The variable temperature magnetic susceptibility data indicate single-ion anisotropy and very weak antiferromagnetic exchange. The tetrahedral environment of Co^{2+} was confirmed by UV-visible spectroscopy. The Co-complex tested by *in vitro* antimicrobial and antioxidant activity shows satisfactory results with an enhancement of activity by complexing the metal with the ligand. In review, such biological activities testing results reveal that the cobalt based complex possess higher activity compared to the parent ligand.

CRediT authorship contribution statement

Sandra Walha: Writing – original draft, Formal analysis. **Noureddine Mhadhbi:** Writing – original draft, Formal analysis. **Basem F. Ali:** Investigation, Data curation, Conceptualization. **Abdellah Kaiba:** Investigation, Data curation, Conceptualization. **Ahlem Guesmi:** Visualization, Formal analysis, Data curation. **Wesam Abd El-Fattah:** Visualization, Formal analysis, Data curation. **Naoufel Ben Hamadi:** Visualization, Formal analysis, Data curation. **Mark M. Turnbull:** Writing – review & editing, Validation, Conceptualization, Data curation. **Ferdinando Costantino:** Supervision, Methodology, Conceptualization. **Houcine Naïli:** Supervision, Methodology, Conceptualization.

Declaration of competing interest

The authors declare that they have no known competing financial interests or personal relationships that could have appeared to influence the work reported in this paper.

Data availability

No data was used for the research described in the article.

Acknowledgements

This work was supported and funded by the Deanship of Scientific Research at Imam Mohammad Ibn Saud Islamic University (IMSIU) (grant number IMSIU-RPP2023025).

Supplementary materials

CCDC 939072 contains the supplementary crystallographic data for this paper. These data can be obtained free of charge via www.ccdc.cam.ac.uk/data_request/cif, by e-mailing data_request@ccdc.cam.ac.uk, or by contacting The Cambridge Crystallographic Data centre, 12 Union Road, Cambridge CB2 1EZ, UK; fax: +44(0)1223-336033.

Supplementary material associated with this article can be found, in the online version, at doi:10.1016/j.chphi.2024.100597.

References

[1] H. Shi, Y. Shan, M. He, Y. Liu, Impetus for solvothermal synthesis technique: synthesis and structure of a novel 1-D borophosphate using ionic liquid as medium, J. Solid State Chem. 176 (1) (2003) 33–36.
[2] A. Stein, S.W. Keller, T.E. Mallouk, Turning down the heat: design and mechanism in solid-state synthesis, Science 259 (5101) (1993) 1558–1564.
[3] J. Gopalakrishnan, Chimie douce approaches to the synthesis of metastable oxide materials, Chem. Mater. 7 (7) (1995) 1265–1275.
[4] A. Yeganeh-Haeri, D.J. Weidner, J.B. Parise, Elasticity of α-cristobalite: a silicon dioxide with a negative Poisson's ratio, Science 257 (5070) (1992) 650–652.
[5] M.E. Davis, R.F. Lobo, Zeolite and molecular sieve synthesis, Chem. Mater. 4 (4) (1992) 756–768.
[6] R.N. Devi, E. Burkholder, J. Zubieta, Hydrothermal synthesis of polyoxotungstate clusters, surface-modified with M (II)-organonitrogen subunits, Inorg. Chim. Acta 348 (2003) 150–156.
[7] R. Visbal, M.C. Gimeno, N-heterocyclic carbene metal complexes: photoluminescence and applications, Chem. Soc. Rev. 43 (10) (2014) 3551–3574.
[8] F. Marchetti, R. Pettinari, C. Pettinari, Recent advances in acylpyrazolone metal complexes and their potential applications, Coord. Chem. Rev. 303 (2015) 1–31.
[9] J. Masternak, M. Zienkiewicz-Machnik, M. Kowalik, A. Jabłońska-Wawrzycka, P. Rogala, A. Adach, B. Barszcz, Recent advances in coordination chemistry of metal complexes based on nitrogen heteroaromatic alcohols. Synthesis, structures and potential applications, Coord. Chem. Rev. 327 (2016) 242–270.
[10] K. Sumida, D.L. Rogow, J.A. Mason, T.M. McDonald, E.D. Bloch, Z.R. Herm, T. H. Bae, J.R. Long, Carbon dioxide capture in metal–organic frameworks, Chem. Rev. 112 (2) (2012) 724–781.
[11] H. Mutlu, C.M. Geiselhart, C. Barner-Kowollik, Untapped potential for debonding on demand: the wonderful world of azo-compounds, Mater. Horiz. 5 (2) (2018) 62–183.
[12] A. Mukherjee, D. Milstein, Homogeneous catalysis by cobalt and manganese pincer complexes, ACS Catal. 8 (12) (2018) 11435–11469.
[13] M.C. Heffern, N. Yamamoto, R.J. Holbrook, A.L. Eckermann, T.J. Meade, Cobalt derivatives as promising therapeutic agents, Curr. Opin. Chem. Biol. 17 (2) (2013) 189–196.
[14] N. Moutia, A. Oueslati, M.B. Gzaiel, K. Khirouni, Crystal structure and AC conductivity mechanism of [N (C3H7)4]2CoCl4 compound, Phys. E Low-Dimens. Syst. Nanostruct. 83 (2016) 88–94.
[15] A. Oulmidi, S. Radi, A. Idir, A. Zyad, I. Kabach, M. Nhiri, K. Robeyns, A. Rotaru, Y. Garcia, Synthesis and cytotoxicity against tumor cells of pincer N-heterocyclic ligands and their transition metal complexes, RSC Adv. 11 (55) (2021) 34742–34753.
[16] J.R. Jiménez, B. Xu, H. El Said, Y. Li, J. von Bardeleben, L.M. Chamoreau, R. Lescouëzec, S. Shova, D. Visinescu, M.G. Alexandru, Field-induced single ion magnet behaviour of discrete and one-dimensional complexes containing [bis (1-methylimidazol-2-yl) ketone]-cobalt (II) building units, Dalton Trans. 50 (44) (2021) 16353–16363.
[17] A. Kumar, P. Yadav, M. Majdoub, I. Saltsman, N. Fridman, S. Kumar, A. Kumar, A. Mahammed, Z. Gross, Corroles: the hitherto elusive parent macrocycle and its metal complexes, Angew. Chem. Int. Ed. Engl. 60 (47) (2021) 25097–25103.

[18] E.M. Johnson, J.J. Liu, A.D. Samuel, R. Haiges, S.C. Marinescu, Switching catalyst selectivity via the introduction of a pendant nitrophenyl group, Inorg. Chem. 61 (3) (2022) 1316–1326.
[19] V.N. Setty, W. Zhou, B.M. Foxman, C.M. Thomas, Subtle differences between Zr and Hf in early/late heterobimetallic complexes with cobalt, Inorg. Chem. 50 (10) (2011) 4647–4655.
[20] O. Ben Moussa, H. Chebbi, M.F. Zid, Crystal structure and Hirshfeld surface analysis of bis (2, 6-diaminopyridinium) tetrachloridocobaltate (II), Acta Crystallogr. E 74 (4) (2018) 436–440.
[21] O.T. Qazvini, V.J. Scott, L. Bondorf, M. Ducamp, M. Hirscher, F.X. Coudert, S. G. Telfer, Flexibility of a metal–organic framework enhances gas separation and enables quantum sieving, Chem. Mater. 33 (22) (2021) 8886–8894.
[22] C. Krebs, I. Jess, C. Näther, Synthesis, crystal structure and thermal properties of bis (1, 3-dicyclohexylthiourea-κS) bis (isothiocyanato-κN) cobalt (II), Acta Crystallogr. E 78 (1) (2022) 71–75.
[23] M. Kandhaswamy, V. Srinivasan, Synthesis and characterization of tetraethylammonium tetrachlorocobaltate crystals, Bull. Mater. Sci. 25 (2002) 41–45.
[24] M. Tahenti, S. Gatfaoui, N. Issaoui, T. Roisnel, H. Marouani, A tetrachlorocobaltate (II) salt with 2-amino-5-picolinium: synthesis, theoretical and experimental characterization, J. Mol. Struct. 1207 (2020) 127781.
[25] M. Said, H. Boughzala, Synthesis, crystal structure, vibrational study, optical properties and thermal behavior of a new hybrid material bis (3-amino-4-phenyl-1H-pyrazolium) tetrachloridocobaltate (II) monohydrate, J. Mol. Struct. 1203 (2020) 127413.
[26] M. Maha, D.E. Janzen, R. Mohamed, S. Wajda, Synthesis, crystal structure, thermal analysis, spectroscopic, and magnetic properties of a novel organic cation tetrachlorocobaltate (II), J. Supercond. Nov. Magn. 29 (2016) 1573–1581.
[27] J.C. Chang, W.Y. Ho, I.W. Sun, Y.K. Chou, H.H. Hsieh, T.Y. Wu, Synthesis and properties of new tetrachlorocobaltate (II) and tetrachloromanganate (II) anion salts with dicationic counterions, Polyhedron 30 (3) (2011) 497–507.
[28] T. Sun, S. Feng, B. Lu, Q. Cai, Ionothermal synthesis in an ionic liquid and crystal structure of $[C_4H_{12}N_2][CoCl_4]$, J. Chem. Res. 40 (8) (2016) 475–477.
[29] W.Q. Chen, M.H. Feng, D.D. Zhou, Y.Q. Peng, S. Han, X.P. Liu, L.M. Yang, J. R. Zhou, C.L. Ni, Two tetrachlorocobaltate (II) salts with substituted benzyl triphenylphosphonium: syntheses, crystal structures, weak interactions, and magnetic properties, Synth. React. Inorg. Met. Org. Chem. 42 (6) (2012) 811–817.
[30] R.D. Willett, C.J. Gómez-García, B. Twamley, Structure and magnetic properties of $[(REDA)Cl]_2CuCl_4$ salts: a new series of ferromagnetic layer perovskites, Polyhedron 24 (2005) 2293–2298.
[31] I. Baccar, F. Issaoui, F. Zouari, M. Hussein, E. Dhahri, M. Valente, Magneto-structural studies of the bis (1, 4-bis (3-aminopropylamine) piperazinium) chloride pentachlorocuprate (II) trihydrate, Solid State Commun. 150 (2010) 2005–2010.
[32] S. Bouacida, R. Bouchene, A. Khadri, R. Belhouas, H. Merazig, Bis [4-(dimethylamino) pyridinium] tetrachloridocuprate (II), Acta Crystallogr. E 69 (11) (2013) m610–m611.
[33] C.S. Hawes, C. Chen, A. Tran, D.R. Turner, Hydrogen-bonding motifs in piperazinediium salts, Crystals 4 (1) (2014) 53–63.
[34] N. Prabavathi, A. Nilufer, V. Krishnakumar, FT-IR, FT-Raman and DFT quantum chemical study on the molecular conformation, vibrational and electronic transitions of 1-(m-(trifluoromethyl) phenyl) piperazine, Spectrochim. Acta A Mol. Biomol. Spectrosc. 121 (2014) 483–493.
[35] A. Gannouni, H. Louis, T. Roisnel, E.E. Ekereke, D.E. Charlie, E. Ukwenya, R. Kefi, Synthesis, X-ray crystallography, spectroscopic characterization, electronic structure investigation and molecular docking studies of single Cobalt (II) metal complex against, J. Mol. Struct. 1203 (2022) 127.
[36] M. Maha, D.E. Janzen, R. Mohamed, S. Wajda, Crystal Structure Synthesis, Thermal analysis, spectroscopic, and magnetic properties of a novel organic cation tetrachlorocobaltate(II), J. Supercond. Nov. Magn. 29 (2016) 1573–1581.
[37] C. Decaroli, A.M. Arevalo-Lopez, C.H. Woodall, E.E. Rodriguez, J.P. Attfield, S. F. Parker, C. Stock, (C4H12N2) [CoCl4]: tetrahedrally coordinated Co2+ without the orbital degeneracy, Acta Crystallogr. Sect. B Struct. Sci. Cryst. Eng. Mater. 71 (2015) 20–24.
[38] M. Mghandef, H. Boughzala, 1-(4-Hydroxyphenyl)piperazine-1,4-diium tetrachloridocobalt(II) monohydrate, Acta Crystallogr. Sect. E Struct. Rep. Online 70 (2014) 0–7.
[39] M. Landolsi, S. Abid, Crystal structure and Hirshfeld surface analysis of trans-2,5-dimethylpiperazine-1,4-diium tetrachloridocobaltate(II), Acta Crystallogr. Sect. E Crystallogr. Commun. 77 (2021) 424–427.
[40] APEX3, Bruker AXS Inc, Madison, Wisconsin, USA, 2015.
[41] SAINT v8.34A, Bruker AXS Inc, Madison, Wisconsin, USA, 2013.
[42] SADABS, v2014/5, Bruker AXS Inc, Madison, Wisconsin, USA, 2014.
[43] L.J. Farrugia, WinGX and ORTEP for windows: an update, J. Appl. Crystallogr. 45 (4) (2012) 849–854.
[44] G.M. Sheldrick, SHELXT - integrated space-group and crystal-structure determination, Acta Crystallogr. A 71 (Pt 1) (2015) 3–8.
[45] G.M. Sheldrick, Crystal structure refinement with SHELXL, Acta Crystallogr. C 71 (Pt 1) (2015) 3–8.
[46] R.L. Carlin, Magnetochemistry, Springer Science & Business Media, 2012.
[47] O.Y. Celiktas, E. Bedir, F.V. Sukan, *In vitro* antioxidant activities of Rosmarinus officinalis extracts treated with supercritical carbon dioxide, Food Chem. 101 (4) (2007) 1457–1464.
[48] G. Sacchetti, S. Maietti, M. Muzzoli, M. Scaglianti, S. Manfredini, M. Radice, R. Bruni, Comparative evaluation of 11 essential oils of different origin as functional antioxidants, antiradicals and antimicrobials in foods, Food Chem. 91 (4) (2005) 621–632.
[49] A. Brace, N.D. Tommasi, L.D. Bari, C. Pizza, M. Politi, I. Morelli, Antioxidant principles from bauhinia terapotensis, J. Nat. Prod. 64 (2001) 892–895.
[50] A. Hachani, I. Dridi, S. Elleuch, T. Roisnel, R. Kefi, Crystal structure, spectroscopic and biological study of a new inorganic-organic hybrid compound $[Cd_4Cl_{12}(H_2O)_2]_n$ $(C_{10}N_4H_{28})_n$, Inorg. Chem. Commun. 100 (2019) 134–143.
[51] F. Garci, H. Chebbi, N. Rouzbeh, L. Rochels, S. Disch, A. Klein, M.F. Zid, Structure, optical and magnetic properties of the pyridinium cobaltate $(C_6H_9N_2)_2[CoCl_4]$, Inorg. Chim. Acta 539 (2022) 121003.
[52] A.N. Protsenko, O.G. Shakirova, A.E. Protsenko, N.V. Kuratieva, S. Fowles, M. M. Turnbull, Effect of isomeric cations of 3(2)-(chloromethyl)pyridine on the structure and properties of copper(II) and cobalt(II) complexes, J. Mol. Struct. 1240 (2021) 130561.
[53] S. Walha, H. Naili, S. Yahyaoui, T. Mhiri, 1-Methylpiperazine-1,4-diium tetrachloridozincate hemihydrate, Acta Crystallogr. E 67 (11) (2011) m1605.
[54] A.M. Ben Salah, S. Walha, S. Yahyaoui, M. Abdalrahman, M.M. Turnbull, M. M, T. Mhiri, H. Naïli, H, Crystal growth, thermal and magnetic characterizations of a new ferromagnetic Ni (II) dimer, Monatsh. Chem. 145 (2014) 1575–1581.
[55] C.H. Peng, Bis (1-methylpiperazine-1, 4-diium) tetrabromidocuprate (II), Acta Crystallogr. E 67 (7) (2011) m967.
[56] C.H. Peng, Bis (1-methylpiperazine-1, 4-diium) tetrachloridocuprate (II), Acta Crystallogr. E 67 (7) (2011) m979.
[57] P.R. Spackman, M.J. Turner, J.J. McKinnon, S.K. Wolff, D.J. Grimwood, D. Jayatilaka, M.A. Spackman, CrystalExplorer: a program for Hirshfeld surface analysis, visualization and quantitative analysis of molecular crystals, J. Appl. Crystallogr. 54 (3) (2021) 1006–1011.
[58] O. Kahn, Molecular Magnetism, VCH Publ. Inc., New York, NY, USA, 1993, p. 393.
[59] P.W. Anderson, Theory of magnetic exchange interactions: exchange in insulators and semiconductors, in: Solid State Physics, 14, Elsevier, 1963, pp. 99–214.
[60] N. Kupko, K.L. Meehan, F.E. Witkos, H. Hutcheson, J.C. Monroe, C.P. Landee, D. A. Dickie, M.M. Turnbull, F. Xiao, Cobalt halide complexes of 2-, 3-and 4-methoxyaniline: syntheses, structures and magnetic behavior, Polyhedron 187 (2020) 114680.
[61] O. Kahn, J. Larionova, J. Yakhmi, Molecular magnetic sponges, Chem. Eur. J. 5 (12) (1999) 3443–3449.
[62] M.L. Mrad, S. Belhajsalah, M.S.M. Abdelbaky, S. García-Granda, K. Essalah, C. B. Nasr, Synthesis, crystal structure, vibrational, optical properties, and a theoretical study of a new Pb (II) complex with bis (1-methylpiperazine-1, 4-diium):$[C_5H_{14}N_2]_2PbCl_6{\cdot}3H_2O$, J. Coord. Chem. 72 (2) (2019) 358–371.
[63] C. Decaroli, A.M. Arevalo-Lopez, C.H. Woodall, E.E. Rodriguez, J.P. Attfield, S. F. Parker, C. Stock, (C4H12N2)[CoCl4]: tetrahedrally coordinated Co2+ without the orbital degeneracy, Acta Crystallogr. B 71 (2015) 1–5.
[64] N. Mhadhbi, S. Said, S. Elleuch, H. Naili, Crystal structure, spectroscopy, DFT studies and thermal characterization of Cobalt(II) complex with 2-protonated aminopyridinium cation as ligand, J. Mol. Struct. 1108 (2016) 223–234.
[65] H. Tllili, S. Walha, H. Naili, S. Elleuch, B.F. Ali, Structural, vibrational, DFT and optical studies of a new non-centrosymmetric hybrid material (C4H12N2)[CoBr4], J. Mol. Struct. 1152 (2017) 303–310.
[66] H. Tlili, S. Walha, S. Elleuch, B. Ali, H. Awad, P. Myllyperkiö, J. Konu, H. Naïli, Electronic studies, biological activities and nonlinear optical properties of a new non-centrosymmetric piperazinediium tetrabromidozincate(II), J. Iran. Chem. Soc. 19 (3) (2022) 763–774.
[67] A. Gannouni, I. Dridi, S. Elleuch, L. Jouffret, R. Kefi, Synthesis and characterization of a hybrid material $(C_{10}H_{28}N_4)[CoCl_4]_2$ using Hirshfeld surface, vibrational and optical spectroscopy, DFT calculations and biological activities, J. Mol. Struct. 1250 (2022) 131804.
[68] N. Hamdi, S. Chaouch, I. da Silva, M. Ezahri, M. Lachkar, R. Alhasan, A.Y. Abdin, C. Jacob, B.E. Bali, Synthesis, structural characterization, and biological activities of organically templated cobalt phosphite $(H_2DAB)[Co(H_2PO_3)4]{\cdot}2H_2O$, Sci 4 (1) (2022) 5.
[69] M. Hartmann, M. Berditsch, J. Hawecker, M.F. Ardakani, D. Gerthsen, A.S. Ulrich, Damage of the bacterial cell envelope by antimicrobial peptides gramicidin S and PGLa as revealed by transmission and scanning electron microscopy, Antimicrob. Agents Chemother. 54 (8) (2010) 3132–3142.
[70] A. Marcu, A. Stanila, O. Cozar, L. David, Structural investigations of some metallic complexes with threonine as ligand, J. Optoelectron. Adv. Mater. 10 (4) (2008) 830–833.
[71] A. Mishra, N.K. Kaushik, A.K. Verma, R. Gupta, Synthesis, characterization and antibacterial activity of cobalt (III) complexes with pyridine–amide ligands, Eur. J. Med. Chem. 43 (10) (2008) 2189–2196.